Solid-State Microcoolers and Thermal Energy Harvesting Microsystems

L.M. Goncalves , R. P. Rocha, J.P. Carmo, J.H. Correia
Electronics Department, University of Minho
lgoncalves@dei.uminho.pt

***Abstract*-A thermoelectric planar microcooler was fabricated on top of a flexible substrate, using Bi_2Te_3 and Sb_2Te_3 thermoelectric elements. Finite element analysis and theoretical calculations previewed a temperature drop of 16 ºC in the cold area of the device. Bi_2Te_3 and Sb_2Te_3 materials were deposited by thermal co-evaporation on a kapton substrate, 12 µm thick. Photolithography and wet-etching were used to patterning the structures. Devices were tested by infrared imaging and results demonstrated that microsystems technology can be applied in the fabrication of thermoelectric microcoolers.**

I. INTRODUCTION

Thermoelectric microcoolers and their integration with microelectronic circuits are in demand for temperature control of small areas, with fast transient response. Since these devices [1,2] are reversible, they can also be used as thermoelectric generators, converting thermal energy into electrical energy [3,4]. Micro-thermoelectric generators can be used in a lot of small, low-power devices such as hearing aids or wrist watches.

Large devices (more than 1 cm^2 area) are commercialized for some years. However, the mechanical processes for their fabrication cannot be used for the fabrication of microscale devices (less then 1 mm^2 area).

The conventional thermoelectric cooler (Fig.1), with the heat flux perpendicular to hot and cold areas, cannot be scalable to microchip dimensions, using the same fabrication methods used for macro-scale devices. New microsystems technology must be used instead, based on thick/thin film technology [5]. Deposition and pattern processes of such films (tens to hundreds of micrometers) are still under development, and a long deposition time is necessary to achieve good materials. The fabrication of the top contact is also an issue on these devices, due to its bridge structure [6], however, Böttner et al. avoided top contact constrains by using two wafers glued [7].

A new design topology was tested in this work. A thin-film planar device, as shown in Fig 2 has lower heat-pump capacity, but a simplified fabrication process [8], since all contacts are in the same plane. The cold area is available in the centre of the device.

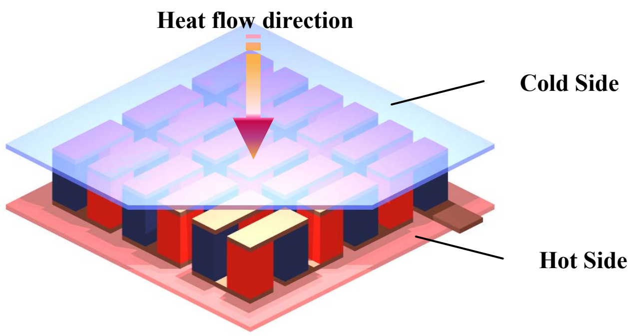

Fig. 1: Conventional thermoelectric device.

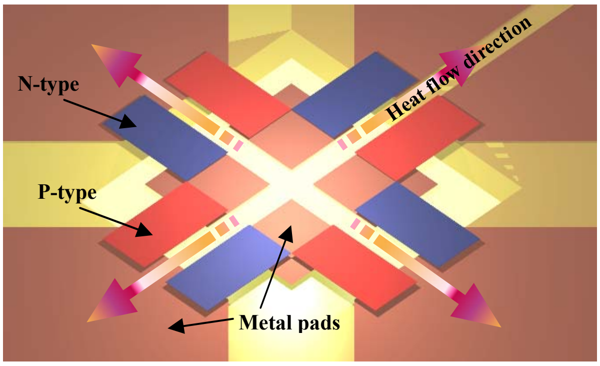

Fig. 2: Planar thermoelectric device.

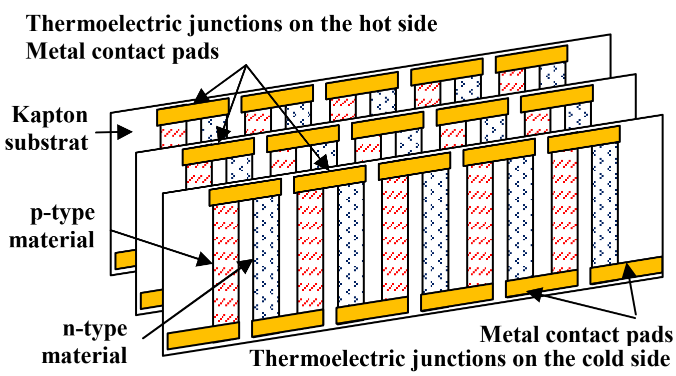

Fig. 3: Artwork of a thermoelectric device with a large number of junctions, optimized energy harvesting.

Using the same planar concept, the fabrication of a thermoelectric generator can also be simplified, as represented in Fig. 3. A large tape with thermoelectric junctions is fabricated by a planar process. This tape is sliced in small strips and connected together as in Fig 3 with all the thermoelectric junctions connected in series. This process allows the fabrication of longer thermoelectric elements, required in some low temperature energy harvesting applications, where a few millimeters of length could be necessary.

II. MODEL

Since each thermoelectric pair can produce a voltage near 400 μV/ºC, many pairs, connected in series, are necessary to generate a usable voltage. The maximum power in a thermoelectric generator, calculated with Eq 1, is obtained when the load resistance equals the internal resistance (R).

$$P_{MAX} = \frac{V_{OUT}^2}{4R} = \frac{\left(n\left(\alpha_p - \alpha_n\right)\Delta T\right)^2}{4n\left(R_n + R_p + R_j + 4R_c\right)} \quad \textbf{(1)}$$

n is the number of elements (pairs of thermoelectric p-n junctions), α is the Seebeck coefficient, ΔT is the temperature difference between the hot side and cold side of thermoelectric elements and R is the electric resistance. The indexes p and n refer to p-type and n-type materials respectively and the indexes j and c refer to materials of contacts and the contact itself. To obtain maximum power, it's also important do match the thermal resistance of the generator with the heatsink (on the cold side) and hot object (in the hot side), not represented in the previous equation. In several applications is also important to analyze the impact of the generator in the temperature of the hot object. If a human-body generator is designed, it will not suit comfortable if much thermal power is absorbed from the skin (the sensation of cold will be noticed). By other hand, when designing a thermoelectric generator for waste heat recovering (ex. recovering heat from a laptop CPU), an increase of temperature could occur where the heat is generated.

The efficient of this generator is calculated with Eq. 2. [9]

$$\Phi_{\max} = \frac{q_C}{W} = \frac{T_1\left[\left(1 + ZT_M\right)^{\frac{1}{2}} - \frac{T_2}{T_1}\right]}{\left(T_2 - T_1\right)\left[\left(1 + ZT_M\right)^{\frac{1}{2}} + 1\right]} \quad \textbf{(2)}$$

Z represents the figure of merit of the device, calculated by Eq. 3, T_1 and T_2 are the temperatures at hot and cold sides and T_M is the mean temperature: $(T_1+T_2)/2$. Despite using figure-of-merit to quantify the quality of a thermoelectric material, this parameter is also used to quantify the performance of a thermoelectric device.

$$Z = \frac{(\alpha_p - \alpha_n)^2}{4\lambda\rho + 8\lambda\rho_c \frac{H}{LL_c} + 4\lambda_m\rho\frac{H_m}{H} + 8\lambda_m\rho_c\frac{H_m}{LL_c} + 4\rho\gamma\frac{L\ell}{H} + 8\rho_c\gamma\frac{\ell}{L_c}} \quad \textbf{(3)}$$

L and H, are respectively length and height of thermoelectric materials. L_c is the length of contacts between TE material and metal pads, ℓ is the length of cold area, α is Seebeck coefficient, ρ electrical resistivity, λ thermal conductivity and ρ_c contact electrical resistivity. The device is supported by an isolating membrane, with thickness H_m, and thermal conductivity λ_m. γ represents a coefficient to include radiation and convection losses, in the range $5 < \gamma < 10$ $\mathrm{Wm^{-2}K^{-1}}$.

The maximum temperature difference that can be obtained, between the hot side and cold side (T_h - T_c), without external load ($Q_L = 0$) is calculated by Eq. 4:

$$\Delta T_{\max} = \frac{1}{2} Z T_c^{\ 2} \quad \textbf{(4)}$$

This maximum temperature difference is obtained when the current (I) has a specific value I_{opt}, as:

$$\frac{\partial T_c}{\partial I} = 0 \Leftrightarrow I_{opt} = \frac{\left(\alpha_p - \alpha_n\right)T_c}{R} \quad \textbf{(5)}$$

And the minimum temperature on the cold side is calculated by eq. 6

$$T_c = \frac{1}{Z}\left(\sqrt{1 + 2ZT_h} - 1\right) \;,\quad I = I_{opt} \quad \textbf{(6)}$$

The previous equations can be used to predict the effect of reducing dimensions of a planar thermoelectric device, from millimeters to micrometers. The graph of Fig 4 presents the effect of scaling down the dimensions of devices, in XY plane. The scale factor $f = 1$ (in horizontal axis) represents a device with dimensions L=W =1 mm, H =10 μm and H_m =10 μm. Lower values of f represents devices where dimensions (L and W) were reduced by a factor f.

© IEEE 2009

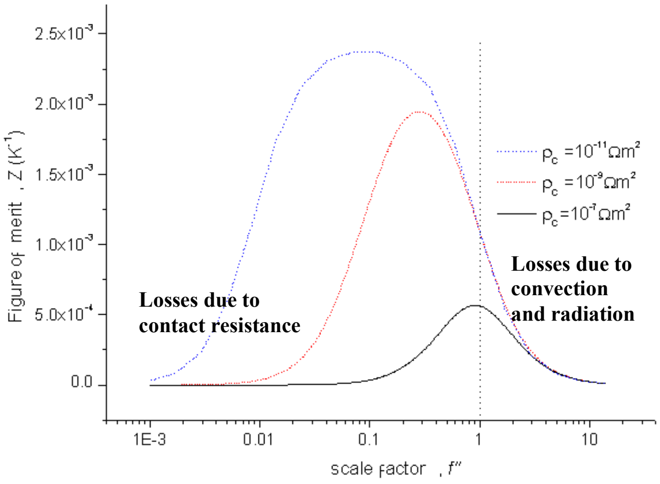

Fig. 4: Effect of scaling the device in XY plane. The height of device and support membrane are constant (H =10 µm and Hm =10µm), while other dimensions are scaled by the value on horizontal axis.

Since the losses by radiation and convection are less relevant in lower dimension devices, figure-of-merit increases when device is smaller. However, a low contact resistivity must be ensured, to keep this higher figure-of-merit. Considering both effects, an optimum dimension exists where figure-of-merit is maximized.

Fig 5 presents the complete model of a thermoelectric device [10], including thermal and electric domains.

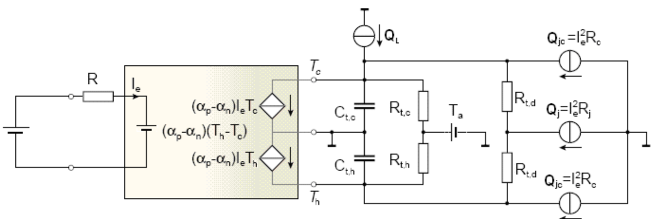

Fig. 5: Complete model of a Peltier microcooler, including electrical and thermal domains.

The electrical model (on the left of Fig 5), includes the electrical equivalent resistance of the device (R), a voltage source that provides power to the device and a voltage source modelling the Seebeck effect of junctions, $(\alpha_p - \alpha_n)(T_h - T_c)$. The resultant current is I_e. On the right side of Fig 5, thermal model is presented. The two current sources, $(\alpha_p - \alpha_n)I_eT_c$ and $(\alpha_p - \alpha_n)I_eT_h$, represent the cooling and heating by Peltier effect, respectively. The capacitors $C_{t,c}$ and $C_{t,h}$ are the heat capacity of on cold side and hot side and resistances $R_{t,c}$ and $R_{t,h}$ are the losses by convection and radiation to ambient temperature, T_a. $R_{t,h}$ is usually very small, and $T_h \approx T_a$. $R_{t,d}$ represents half of the thermal resistance between hot side and cold side, including support membrane effects. Q_j and Q_{jc} represent the heating by Joule, respectively on the thermoelectric materials and contacts. The load applied on the cold side of the device is represented by Q_L.

A thermoelectric cooler can be analyzed using finite element modelling. After designing the structure, two type of loads are considered:

1. *Peltier effect on hot and cold sides.*

The cooling by Peltier effect is calculated with Eq 7 and the heating with Eq 8. (T_C represents the temperature on the cold side and T_H the temperature on the hot side)

$$Q_c = Q_{nc} + Q_{pc} = (\pi_n + \pi_p)I = (\alpha_p - \alpha_n)T_c I \quad \textbf{(7)}$$

$$Q_h = Q_{nh} + Q_{ph} = (\pi_n + \pi_p)I = (\alpha_p - \alpha_n)T_h I \quad \textbf{(8)}$$

This load is applied p-n junction of the device. Q_C should be negative, since heat is removed in the cold side of the device.

2. *Joule heating*

Joule heating should be considered in all electrical resistances of the device. This includes the p and n materials, the metallic contact between them and the interface contact resistances. The metallic contact resistance is usually neglected, since the value is very small compared with p and n materials, due to its low resistivity. Eq 9 calculates the total equivalent resistance of a thermoelectric p-n pair. W is the width of elements and the other symbols are as defined in Eq 3.

$$R_{eq} = R_e + 2R_c = \rho_n \frac{L_n}{W_n H_n} + \rho_p \frac{L_p}{W_p H_p} + 2\left(\frac{\rho_{cn}}{L_c W_n} + \frac{\rho_{cp}}{L_c W_p}\right) \quad \textbf{(9)}$$

Joule heating should be calculated and applied in these volumes. Convection and radiation should be considered in all surfaces. Fig 6 shows the surface temperature of a planar Peltier microcooler, on top of a Kapton polyimide substrate. A temperature difference of 16 ºC (between hot side and cold side) was obttained in simulation results [11].

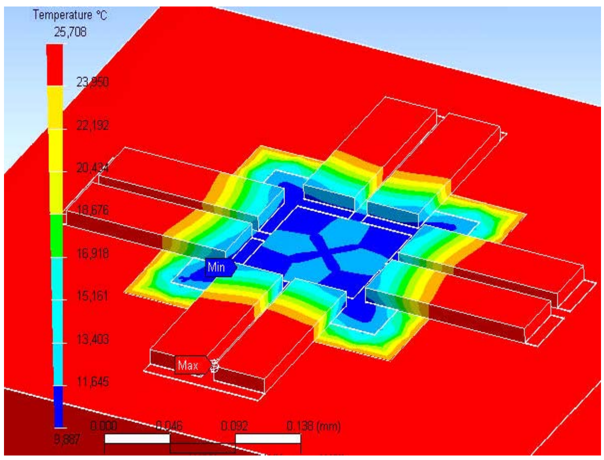

Fig. 6: FEM simulation of a microdevice shows the possibility of achieving a temperature difference between hot and cold sides of 16 ºC

III. Materials and Processes

Bismuth, antimony and tellurium compounds (Bi_2Te_3 Sb_2Te_3) are the best materials to fabricate thermoelectric converters. These materials were used for many years to fabricate large thermoelectric devices and are also used in this work, in form of thin-films.

Sputtering (from compound targets) or co-sputtering (from single-element targets), metal-organic chemical vapour deposition (MOCVD), electrochemical deposition (ECD) and thermal evaporation were used before to fabricate thermoelectric films of Bi_2Te_3 and Sb_2Te_3. Some of these techniques achieve good thermoelectric properties, but deposition rate is very slow. Others require very expensive equipment. The thermal co-evaporation (with heated substrate) used in this work proved to be a cost-effective technique to obtain thermoelectric properties as good as the best reported for the same materials.

The conventional structure presented in Fig. 1 requires a substrate with high thermal conductivity, to thermal-connect the hot and cold side of the device respectively with a heatsink and the cooling load. Since this substrate should also be electrical insulating, ceramics are usually used in large scale devices and Si with SiO_2 layer in microdevices. In the other way, the planar device of Fig. 2 requires a thermal and electrical isolating substrate. For this reason, Kapton polyimide substrate (25 μm thickness) was chosen. Moreover, this substrate presented superior adhesion and lower intrinsic stress than glass or silicon. Using the device as a generator (Fig. 3) kapton substrate doesn't create an additional heat-path between hot side and cold side, thus increasing overall efficiency. Table 1 presents the composition, the Seebeck coefficient (α) and electrical resistivity (ρ) of selected films of Bi_2Te_3 and Sb_2Te_3. Thermal conductivity, κ, was measured [12] and the values of 1.3 $Wm^{-1}K^{-1}$ and 1.8 $Wm^{-1}K^{-1}$ were obtained at room temperature, respectively in Bi_2Te_3 and Sb_2Te_3 films.

Table I: Properties of selected films.

Film	***Type***	***%Te by EDX***	***α [μVK^{-1}]***	***ρ [$\mu\Omega m$]***
#282B	Bi_2Te_3	59.1%	-180	7.3
#273C	Bi_2Te_3	62.0%	-248	12.6
#281D	Bi_2Te_3	n.a.	-220	10.6
#304D	Sb_2Te_3	61.2%	133	10.0
#306A	Sb_2Te_3	67.3%	156	9.2
#306D	Sb_2Te_3	73.5%	188	12.6

Telluride films were patterned by wet etching in HNO_3:HCl:H_2O solution. Etch rate was evaluated for difference concentrations, in order to get optimized results. The fabrication steps of such planar devices were presented before [13]. Fig 6 shows a microdevice fabricated by this technique.

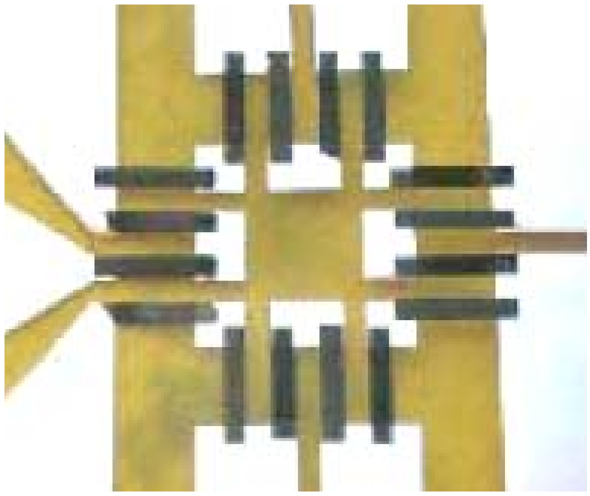

Fig. 7: Planar Peltier microcooler with eight pairs of thermoelectric elements connected in series with aluminum/nickel contact pads.

IV. Results

A microcooler was tested in vacuum, using an infrared microscope. The optimum current (the current that gives the maximum temperature difference) was applied. Fig 8 shows the temperature map obtained in two elements (n-type and p-type) of the microcooler. A temperature difference of 5 ºC was measured between the hot side and the cold side. The achieved temperature difference and the minimum achieved temperature on cold side are far from expected values calculated on simulations. A hot-side-to-cold-side temperature difference of 10 ºC and a cold side to base temperature difference of 5 ºC were expected, in a device with this dimension [8].

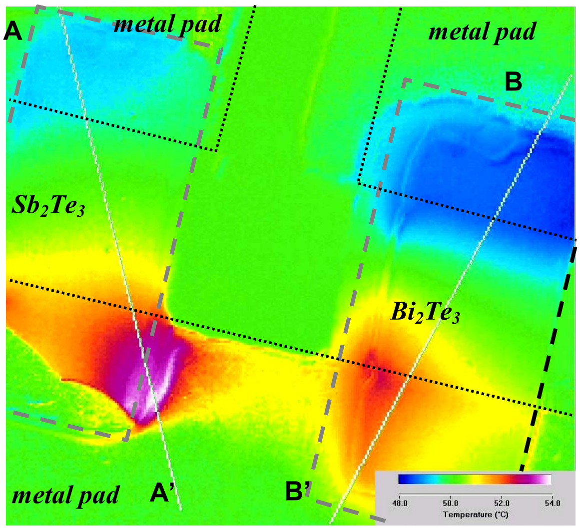

Fig. 8: Thermal image of two legs of the microcooler (each colour represents different temperature).

These differences are due to higher value of the electrical contact resistance than the one used in simulation. A resistance value of 2 Ω was measured between Bi_2Te_3 and metal pad and less than 0.2 Ω between Sb_2Te_3 and metal pad. These values correspond to a contact resistivity of 10^{-2} Ωcm^2 and 10^{-3} Ωcm^2 on a contact area of 0.5 mm^2. Values between 10^{-3} Ωcm^2 and 10^{-6} Ωcm^2 have been reported before [6, 7]. Also the power factor of the thermoelectric films incorporated in the microcooler (1.6×10^{-3} $WK^{-2}m^{-1}$ for n-type and 2.2×10^{-3} $WK^{-2}m^{-1}$ for p-type) were significantly smaller that the best values obtainable for these materials, e.g., 4.9×10^{-3} $WK^{-2}m^{-1}$ for n-type [8]. A generator is also being fabricated, as presented in artwork of Fig. 2.

V. Conclusions

Planar thermoelectric converters were dimensioned for cooling and energy harvesting applications.

Thin film materials with value of figure of merit equivalent to those obtained in bulk materials were deposited by co-evaporation. The values of figure of merit of 0.9 and 0.4 were measured at room temperature, respectively for Bi_2Te_3 and Sb_2Te_3. These values compare well with the best published results for the same materials.

Films were patterned by wet-etching in HNO_3:HCl:H_2O and the influence of the etchant composition in the etch rate and pattern quality was investigated.

A microcooler was fabricated and a temperature difference of 5 ºC was achieved, between the hot and cold side of the device. Apart from the figures of merit of materials, the thermal and electrical contact resistances affect significantly the performance of thermoelectric microcoolers.

These fabrication techniques will be applied in the fabrication of a thermoelectric energy harvesting microsystem.

Acknowledgment

This work was supported by FCT/PTDC/EEA-ENE/66855/2006.

References

[1] G.J. Snyder et al. "Thermoelectric microdevice fabricated by a MEMS like electrochemical process". *Nature Material Letters, 2* (2003) 528.

[2] L. Bell, "Cooling, heating, generating power, and recovering waste heat with thermoelectric systems". *Science, 321,* (2008) 1457.

[3] W. Qu, et al."Microfabrication of thermoelectric generators on flexible foil substrates as a power source for autonomous microsystems". *Journal of Micromechanical and Microengineering, 11*, (2001) 152.

[4] J Caylor, R Venkatasubramanian, "Si/Ge Superlattice Structures for Thermoelectric Power Generation", *American Physical Society, APS March Meeting*, March 5-9, 2007

[5] L. M. Goncalves, J. G. Rocha, C. Couto, P. Alpuim, Gao Min, D.M. Rowe J.H. Correia, "Fabrication of flexible thermoelectric microcoolers using planar thin-film technologies" *Journal of Micromechanical and Microengineering 17* (2007)

[6] L.W. da Silva, M. Kaviany," Fabrication and measured performance of a first-generation microthermoelectric cooler". *Journal of Memscience, 14(5)*, 1110.

[7] H. Böttner, et al. "New thermoelectric components using microsystem technologies". *Journal of Microelectromechanical Systems, 13*, (2004). 414-420.

[8] L.M. Goncalves, C. Couto, J.H. Correia, P. Alpuim, Gao Min, D.M. Rowe, "Flexible Thin-film Planar Peltier Microcooler", *ICT'06 International Conference On Thermoelectrics*, Austria 6-10 Aug (2006)

[9] D.M. Rowe (editor) (1987). Handbook of thermoelectrics. CRC Press. 211-237.

[10] D.D.L Wijngaards, S.H. Kong, M. Bartek, R.F. Wolffenbuttel, "Design and fabrication of on-chip integrated polySiGe and polySi Peltier devices", *Sensors & actuators A. Physical, 85* (2000) 316-323.

[11] L.M. Goncalves, J.G. Rocha, C. Couto, P. Alpuim, and J.H. Correia, On-Chip Array of Thermoelectric Peltier Microcoolers, *Sensors and Actuators A: Physical* 145–146 p75–80 (2008)

[12] F. Völklein, in *Proc. Symposium on Microtechnology in Metrology and Metrology in Microsystems*. Delft, The Netherlands (2000).

[13] L M Goncalves, C Couto, P Alpuim and J H Correia "Thermoelectric Micro Converters for Cooling and Energy Scavenging Systems" *Journal of Micromechanical and Microengineering, 18* (2008)